Polyhedron 30 (2011) 2627–2636

Contents lists available at ScienceDirect

Polyhedron

journal homepage: www.elsevier.com/locate/poly

Zinc(II) complexes with novel 1,3-thiazine/pyrazole derivative ligands: Synthesis, structural characterization and effect of coordination on the phagocytic activity of human neutrophils

P. Torres-García [a], E. Viñuelas-Zahínos [a], F. Luna-Giles [a,*], J. Espino [b], F.J. Barros-García [a]

[a] Departamento de Química Orgánica e Inorgánica, Facultad de Ciencias, Universidad de Extremadura, 06071 Badajoz, Spain
[b] Departamento de Fisiología, Facultad de Ciencias, Universidad de Extremadura, 06071 Badajoz, Spain

ARTICLE INFO

Article history:
Received 5 May 2011
Accepted 15 July 2011
Available online 23 July 2011

Keywords:
Thiazine
Pyrazole
Zinc(II) complexes
Crystal structures
Phagocytosis
Human neutrophils

ABSTRACT

The new ligands 2-(1-pyrazolil)-1,3-thiazine (PzTz), 2-(3,5-dimethyl-1-pyrazolil)-1,3-thiazine (DMPzTz) and 2-(3,5-diphenyl-1-pyrazolil)-1,3-thiazine (DPhPzTz) and the complexes $[ZnCl_2(H_2O)(PzTz)]$ (**1**), $[ZnCl_2(DMPzTz)]$ (**2**) and $[ZnCl_2(DPhPzTz)]$ (**3**) have been isolated and then characterized by elemental analysis, IR spectra and UV–Vis spectroscopy. Besides, the crystal structure of ligands PzTz and DPhPzTz and complexes **1**–**3** have been determined by single-crystal X-ray diffraction. In **1**, the geometry around the Zn(II) atom can be considered a highly distorted trigonal bipyramid, with the metallic atom bonded to two chlorine atoms, one water molecule and one bidentate PzTz ligand. In **2** and **3**, the environment around the metal ion can be described as a distorted tetrahedron with the zinc atom coordinated to one bidentate organic ligand molecule and two chloro ligands. In addition, the phagocytic function of human neutrophils treated with complexes **1**–**3**, their organic ligands and $ZnCl_2$ has been evaluated. The activity of cells enhanced in samples treated with **1**, **2** and **3** with respect to the ones to which the inorganic salt, PzTz, DMPzTz or DPhPzTz were added.

1. Introduction

Human neutrophil polymorphonuclear leukocytes play an important role in the innate immune system (cell-mediated defense system) since these cells are able to recognize invading microorganism, migrate to the infected area, incorporate the pathogens into their cytoplasm and degrade them using a chemical process named respiratory burst, by means of which reactive oxygen intermediates, such as superoxide anions, hydrogen peroxide or hydroxyl radicals, are formed. The generation of these reactive species, that are responsible for killing phagocytosed microorganism, is controlled by several enzymes, including NADPH-oxidase, superoxide dismutase, peroxidase and catalase [1,2].

Zinc is an essential trace element for many biological functions, including immune functions [3]. A large number of enzymes depend on zinc for their catalytic activity (e.g. alcohol dehydrogenase, RNA polymerases, NADPH-oxidase, superoxide dismutase) and a deficiency of zinc is associated with loss of the enzymatic activity and impaired immune responses like phagocytic function [4,5]. Thus, the generation of superoxide anion O_2^- from O_2 in phagocytes by means of NADPH oxidase activity is regulated by Zn(II) ion which acts on channels of the neutrophil membrane [6]. Likewise, by its antioxidant capacity, zinc contributes to the protection of cells from the damaging effects of reactive oxygen radicals produced during immune activation [5].

It is well-known that some coordination compounds can interfere with in vitro phagocytosis, either inhibiting it, as it is the case of certain diclofenac transition metal complexes [7], or improving it, like copper(II) and ruthenium(II) complexes [8]. Additionally, it has been proved that some zinc(II) [9], cadmium(II) [10] and copper(II) [11] complexes with several thiazoline or thiazine derivative ligands are able to improve the phagocytic activity of human neutrophils with respect to the untreated samples (control) and the samples treated with the organic ligands.

In this paper we present the synthesis of new ligands 2-(1-pyrazolyl)-1,3-thiazine (PzTz), 2-(3,5-dimethyl-1-pyrazolyl)-1,3-thiazine (DMPzTz) and 2-(3,5-diphenyl-1-pyrazolyl)-1,3-thiazine (DPhPzTz), whose structures contain pyrazole and 1,3-thiazine rings (see Scheme 1). These heterocycles are present in several natural and synthetic products with antimicrobial, analgesic and antiinflammatory properties, examples being celecoxib [12] and the cephalosporins [13]. The ligands have been characterized by elemental analysis, IR spectroscopy, ^1H and ^{13}C NMR spectroscopy and, in the case of PzTz and DPhPzTz, by single crystal X-ray diffraction. Besides, their complexes with Zn(II) have been obtained and structurally characterized by elemental

* Corresponding author. Tel.: +34 924 289 397; fax: +34 924 271 149.
E-mail address: pacoluna@unex.es (F. Luna-Giles).

0277-5387/$ - see front matter © 2011 Elsevier Ltd. All rights reserved.
doi:10.1016/j.poly.2011.07.014

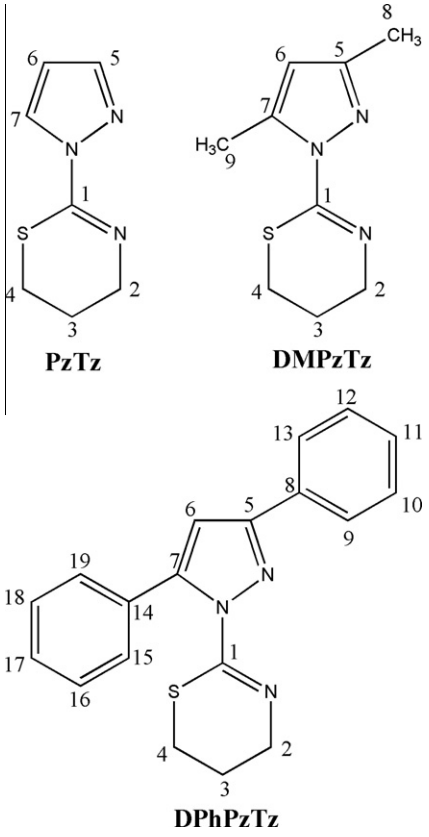

Scheme 1. Synthesis of ligands and zinc(II) complexes.

analysis, IR spectroscopy, X-ray diffraction, UV–Vis spectroscopy and mass spectroscopy. In addition, the influence of the coordination to Zn(II) in the phagocytic activity of human neutrophils was investigated and the results were compared with those obtained for the zinc(II) complex with ligand 2-(3,4-dichlorophenyl)imino-*N*-(4*H*-5,6-dihydro-1,3-thiazin-2-yl)tetrahydro-1,3-thiazine (TzTz), previously reported [9], motivated by the structural resemblance between the complexes studied in this work and [$ZnCl_2$(TzTz)], with the objective of determine whether the type of organic ligand has any influence in the biological activity.

2. Materials and methods

2.1. General procedures

All reagents were commercial grade material and used without any further purification. 3-Chloropropylisothiocyanate was obtained as previously reported [14]. Chemical analyses of carbon, hydrogen, nitrogen and sulfur were performed by microanalytical methods using a Leco CHNS-932 microanalyser. IR spectra were recorded on a Termo IR-300 spectrophotometer, from KBr pellets in the 4000–370 cm^{-1} range and on a Perkin-Elmer FT-IR 1700× spectrophotometer, from Nujol mull in the 500–150 cm^{-1} range. ^{1}H NMR spectra for the organic ligands and their complexes at 400 MHz in $CDCl_3$ and DMSO-d_6, and ^{13}C NMR spectra for the ligands in $CDCl_3$ at 100 MHz were obtained with Bruker AM 400 instrument. Mass spectra for **1**–**3** were performed in a water–DMSO 9:1 v/v mixture. An API ion trap spectrometer (Finnigan LCQ Advantage Max, Thermo Electron Corporation) was used to introduce the samples by syringe pump into the MS detector in the ESI/MS. The MS conditions were: sheath gas flow rate: 10; aux/sweep gas flow rate: 5; spray voltage: 4.5 kV; capillary temperature: 250 °C, capillary voltage: 10.00 V. Electronic spectra in a DMSO solution of the organic ligands and the complexes at a concentration of 10^{-5} M were measured on a Shimadzu UV-3101 PC spectrophotometer using a 10 mm quartz cell.

2.2. Synthesis of the ligands

2.2.1. Synthesis of 2-(1-pyrazolyl)-1,3-thiazine (PzTz)

Sodium hydride 60% (0.600 g, 0.017 mol) was added to a solution of pyrazole (0.695 g, 0.010 mol) in toluene (50 mL). The mixture was stirred at room temperature for 3 h. Then a solution of 3-chloropropylisothiocyanate (1.490 g, 0.010 mol) in toluene (5 mL) was added and the reaction mixture was refluxed for 4 h and cooled. After the addition of methanol (5 mL) the solvent was removed in vacuo. Water was added to the residue and the organic phase was extracted with chloroform, dried with anhydrous Na_2SO_4 and the solvent evaporated. The resulting oil was recrystallized in diethyl ether/petroleum ether 1:1 v/v, obtaining colorless crystals (0.930 g, 55.6%) that were filtered and air-dried. *Anal.* Calc. for $C_7H_9N_3S$: C, 50.27; H, 5.42; N, 25.13; S, 19.17. Found: C, 50.49; H, 5.50; N, 25.24; S, 19.46%. ^{1}H NMR (400 MHz, $CDCl_3$, 25 °C): C(7)H, δ = 8.17 ppm (d, J = 2.8 Hz, 1H); C(5)H, δ = 7.60 ppm (d, J = 0.8 Hz, 1H); C(6)H, δ = 6.34 ppm (m, J = 1.5 Hz, 1H); CH_2–N, δ = 3.81 ppm (t, J = 5.6 Hz, 2H); CH_2–S, δ = 3.11 ppm (t, J = 6.0 Hz, 2H); CH_2, δ = 1.93 ppm (m, J = 5.7 Hz, 2H); ^{1}H NMR (400 MHz, DMSO-d_6, 25 °C): C(7)H, δ = 8.30 ppm (d, J = 2.8 Hz, 1H); C(5)H, δ = 7.68 ppm (s, 1H); C(6)H, δ = 6.48 ppm (d, J = 1.6 Hz, 1H); CH_2–N, δ = 3.77 ppm (t, J = 5.4 Hz, 2H); CH_2–S, δ = 3.15 ppm (t, J = 5.8 Hz, 2H); CH_2, δ = 1.84 ppm (m, J = 5.6 Hz, 2H); ^{13}C NMR (100 MHz, $CDCl_3$, 25 °C): δ = 146.8 ppm C(1); 141.0 ppm C(5); 125.7 ppm C(7); 107.4 ppm C(6); 46.0 ppm C(2), 26.2 ppm C(4), 19.7 ppm C(3). IR(KBr): thiazine ring vibrations 1635 [ν(C=N)], 932, 915, 884, 779, 620, 580, 525, 423 cm^{-1}; pyrazole ring vibrations: 1510, 1419, 1386, 1327, 995 cm^{-1}.

2.2.2. Synthesis of 2-(3,5-dimethyl-1-pyrazolyl)-1,3-thiazine (DMPzTz)

3,5-Dimethylpyrazole (0.961 g, 0.010 mol) was dissolved in toluene (50 mL) and sodium hydride 60% (0.600 g, 0.017 mol) was added. After stirring the mixture for 3 h at room temperature, a solution of 3-chloropropylisothiocyanate (1.490 g, 0.010 mol) in toluene (5 mL) was added. After this, the reaction mixture was heated to reflux for 4 h, cooled, and methanol (5 mL) was added. The solvent was removed under reduced pressure and the residue was washed with water. The organic phase was extracted with chloroform, dried over anhydrous sodium sulfate and treated with activated carbon. After filtration and evaporation a pale yellow oil is obtained (1.18 g, 60.4%). *Anal.* Calc. for $C_9H_{13}N_3S$: C, 59.32; H, 7.19; N, 23.06; S, 17.60. Found: C, 59.01; H, 7.12; N, 22.69; S, 17.31%. ^{1}H NMR (400 MHz, $CDCl_3$, 25 °C): C(6)H, δ = 5.88 ppm (s, 1H); CH_2–N, δ = 3.82 ppm (t, J = 5.6 Hz, 2H); CH_2–S, δ = 3.09 ppm (t, J = 6.0 Hz, 2H); C(8)H_3, δ = 2.43 ppm (s, 3H); C(9)H_3, δ = 2.21 ppm (s, 3H); CH_2, δ = 1.90 ppm (m, J = 5.8 Hz, 2H); ^{1}H NMR (400 MHz, DMSO-d_6, 25 °C): C(6)H, δ = 6.03 ppm (s, 1H); CH_2–N, δ = 3.77 ppm (t, J = 5.6 Hz, 2H); CH_2–S, δ = 3.10 ppm (t, J = 5.6 Hz, 2H); C(8)H_3, δ = 2.40 ppm (s, 3H); C(9)H_3, δ = 2.12 ppm (s, 3H); CH_2, δ = 1.81 ppm (m, J = 5.6 Hz, 2H); ^{13}C NMR (100 MHz, $CDCl_3$, 25 °C): δ = 148.8 ppm C(5); 147.4 ppm C(1); 141.0 ppm C(7); 108.7 ppm C(6); 46.1 ppm C(2), 26.7 ppm C(4), 19.7 ppm C(3); 14.1 ppm C(8); 13.4 ppm C(9). IR(KBr): thiazine ring vibrations 1639 [ν(C=N)], 960, 881, 862, 750, 736, 586 cm^{-1}; pyrazole ring vibrations: 1566, 1411, 1375, 1315, 981 cm^{-1}.

2.2.3. Synthesis of 2-(3,5-diphenyl-1-pyrazolyl)-1,3-thiazine (DPhPzTz)

A solution of 3,5-diphenylpyrazole (2.200 g, 0.010 mol) in toluene (50 mL) was treated with sodium hydride 60% (0.600 g,

0.0170 mol) and the resulting mixture was stirred 3 h at room temperature. Then, a solution of 3-chloropropylisothicyanate (1.490 g, 0.010 mol) in toluene (5 mL) was added. The mixture was refluxed for 4 h and cooled. After addition of 5 mL of methanol, the organic solvent was removed in vacuo and water was added. Extraction with chloroform, drying over anhydrous sodium sulfate and concentration gave a yellow oil. The product was purified by flash chromatography, using a mixture dichloromethane/diethyl ether 20:1 v/v. The early fractions of the chromatography contained DPhPzTz, which was recrystallized in diethyl ether/petroleum ether 1:1 v/v, yielding colorless crystals (1.750 g, 54.8%). *Anal.* Calc. for $C_{19}H_{17}N_3S$: C, 71.44; H, 5.33; N, 13.15; S, 10.04. Found: C, 71.33; H, 5.20; N, 12.80; S, 9.68%. ^{1}H NMR (400 MHz, $CDCl_3$, 25 °C): C(9)H, C(13)H, δ = 7.90 ppm (d, J = 7.6 Hz, 2H); C(19)H, C(15)H, δ = 7.50 ppm (d, J = 7.6 Hz, 2H); C(10–12)H, C(16–18)H, δ = 7.44–7.33 ppm (m, 6H); C(6)H, δ = 6.73 ppm (s, 1H); CH_2–N, δ = 3.69 ppm (t, J = 5.4 Hz, 2H); CH_2–S, δ = 3.18 ppm (t, J = 5.8 Hz, 2H); CH_2, δ = 1.92 ppm (m, J = 5.7 Hz, 2H); ^{1}H NMR (400 MHz, DMSO-d_6, 25 °C): C(9)H, C(13)H, δ = 7.89 ppm (d, J = 8.4 Hz, 2H); C(10–12)H, C(15–19)H, δ = 7.52–7.37 ppm (m, 8H); C(6)H, δ = 7.11 ppm (s, 1H); CH_2–N, δ = 3.59 ppm (t, J = 5.6 Hz, 2H); CH_2–S, δ = 3.24 ppm (t, J = 5.6 Hz, 2H); CH_2, δ = 1.84 ppm (m, J = 5.1 Hz, 2H); ^{13}C NMR (100 MHz, $CDCl_3$, 25 °C): δ = 151.9 ppm C(1); 147.7 ppm C(5); 144.6 ppm C(7); 132.4 ppm C(14); 130.8 ppm C(8); 128.0–128.8 ppm (eight signals) C(9), C(10), C(12), C(13), C(15), C(16), C(18), C(19); 126.0 ppm C(17); 99.9 ppm C(6); 46.8 ppm C(2), 27.1 ppm C(4), 19.3 ppm C(3). IR(KBr): thiazine ring vibrations 1639 [ν(C=N)], 945, 921, 871, 761, 617, 605, 534, 461 cm^{-1}; pyrazole ring vibrations: 1548, 1406, 1303, 998 cm^{-1}.

2.3. Preparation of the complexes

2.3.1. Preparation of [$ZnCl_2(H_2O)$(PzTz] (**1**)

This complex was prepared by reacting an ethanol 96% solution (3 mL) of $ZnCl_2$ (0.081 g, 0.6 mmol) with an ethanol 96% solution (5 mL) of PzTz (0.100 g, 0.6 mmol). The resulting solution was surrounded with ether using a liquid-vapor diffusion method to obtain colorless crystals (0.106 g, 55.5%). The crystals were filtrated, washed with cold ether and air dried. *Anal.* Calc. for $C_7H_{11}Cl_2N_3OSZn$: C, 26.15; H, 3.45; N, 13.07; S, 9.97. Found: C, 26.54; H, 3.30; N, 13.31; S, 10.18%. ^{1}H NMR (400 MHz, DMSO-d_6, 25 °C): C(7)H, δ = 8.30 ppm (d, J = 2.8 Hz, 1H); C(5)H, δ = 7.68 ppm (s, 1H); C(6)H, δ = 6.48 ppm (d, J = 1.5 Hz, 1H); CH_2–N, δ = 3.77 ppm (t, J = 5.6 Hz, 2H); CH_2–S, δ = 3.15 ppm (t, J = 5.8 Hz, 2H); CH_2, δ = 1.85 ppm (m, J = 5.6 Hz, 2H); IR(KBr): thiazine ring vibrations 1625 [ν(C=N)], 954, 917, 889, 790, 777, 646, 607, 530, 418 cm^{-1}; pyrazole ring vibrations: 1525, 1396, 1332, 997 cm^{-1}.

2.3.2. Preparation of [$ZnCl_2$(DMPzTz] (**2**)

$ZnCl_2$ (0.070 g, 0.5 mmol) dissolved in methanol (3 mL) was added to a methanol solution (5 mL) of DMPzTz (0.100 g, 0.5 mmol). The resulting solution was allowed to evaporate slowly at room temperature. After a few days, colorless crystals of considerable size were isolated from the solution (0.119 g, 70.1%). Crystals were separated by filtration, washed with cold ether and finally air dried. *Anal.* Calc. for $C_9H_{13}Cl_2N_3SZn$: C, 32.59; H, 3.92; N, 12.67; S, 9.66. Found: C, 32.44; H, 3.73; N, 12.52; S, 9.36%. ^{1}H NMR (400 MHz, DMSO-d_6, 25 °C): C(6)H, δ = 6.03 ppm (s, 1H); CH_2–N, δ = 3.77 ppm (t, J = 5.2 Hz, 2H); CH_2–S, δ = 3.10 ppm (t, J = 5.6 Hz, 2H); C(8)H_3, δ = 2.40 ppm (s, 3H); C(9)H_3, δ = 2.12 ppm (s, 3H); CH_2, δ = 1.81 ppm (m, J = 5.2 Hz, 2H); IR(KBr): thiazine ring vibrations 1597 [ν(C=N)], 975, 904, 862, 748, 694, 626, 593, 545, 439 cm^{-1}; pyrazole ring vibrations: 1564, 1417, 1380, 1317, 989 cm^{-1}.

2.3.3. Preparation of [$ZnCl_2$(DPhPzTz] (**3**)

This complex was isolated by adding a methanol solution (3 mL) of $ZnCl_2$ (0.043 g, 0.3 mmol) to another methanol solution (15 mL) of DPhPzTz (0.100 g, 0.3 mmol), being obtained colorless crystals after a slow evaporation of the solution at room temperature (0.112 g, 78.6%). The crystals were filtered, washed with cold ether and air dried. *Anal.* Calc. for $C_{19}H_{17}Cl_2N_3SZn$: C, 50.07; H, 3.76; N, 9.22; S, 7.04. Found: C, 49.88; H, 4.08; N, 9.23; S, 6.95%. ^{1}H NMR (400 MHz, DMSO-d_6, 25 °C): C(9)H, C(13)H, δ = 7.89 ppm (d, J = 8.0 Hz, 2H); C(10–12)H, C(15–19)H, δ = 7.52–7.37 ppm (m, 8H); C(6)H, δ = 7.11 ppm (s, 1H); CH_2–N, δ = 3.59 ppm (t, J = 5.4 Hz, 2H); CH_2–S, δ = 3.24 ppm (t, J = 5.8 Hz, 2H); CH_2, δ = 1.83 ppm (m, J = 5.5 Hz, 2H); IR(KBr): thiazine ring vibrations 1635 [ν(C=N)], 946, 916, 877, 757, 613, 599, 536, 487 cm^{-1}; pyrazole ring vibrations: 1548, 1406, 1303, 998 cm^{-1}.

2.4. Crystal structures determination

X-ray diffraction measurements were performed using a Bruker APEX or a Bruker SMART CCD diffractometer with Mo Kα radiation (λ = 0.71073 Å, graphite monochromator). The first 50 frames were measured at the end of the data collection to monitor instrument and crystal stability. Absorption correction were applied using the program SADABS [15]. The structures were solved by direct methods and subsequent Fourier differences using the SHELXS-97 [16] program and refined by full-matrix least-squares on F^2 with SHEXL-97 [17], included in WINGX package [18], assuming anisotropic

Table 1
Crystal data and structure refinement for ligands PzTz and DPhPzTz.

	PzTz	DPhPzTz
Crystal shape	prism	prism
Color	colorless	colorless
Size (mm)	0.46 × 0.43 × 0.21	0.55 × 0.37 × 0.27
Chemical formula	$C_7H_9N_3S$	$C_{19}H_{17}N_3S$
Formula weight	167.23	319.42
Crystal system	triclinic	monoclinic
Space group	$P\bar{1}$	$P2_1/n$
Unit cell dimensions		
a (Å)	9.661(1)	9.141(1)
b (Å)	9.708(1)	37.458(2)
c (Å)	17.478(1)	9.655(1)
α (°)	75.854(2)	
β (°)	76.596(2)	101.203(2)
γ (°)	89.904(2)	
Cell volume (Å^3)	1543.5(1)	3243.1(3)
Z	8	8
T (K)	100(1)	100(1)
D_{calc} (g cm^{-3})	1.439	1.308
μ (mm^{-1})	0.351	0.202
F(0 0 0)	704	1344
θ Range	1.2–26.0	1.1–26.0
Index ranges	$-11 \leqslant h \leqslant 11$, $-11 \leqslant k \leqslant 11$, $0 \leqslant l \leqslant 21$	$-11 \leqslant h \leqslant 11$, $0 \leqslant k \leqslant 46$, $0 \leqslant l \leqslant 11$
Independent reflections	6024	6386
Observed reflections [$F > 4.0\sigma(F)$]	5061	4967
Data completeness	0.994	1
Maximum/minimum transmission	0.930/0.855	0.947/0.897
No. of reflection parameters	397	415
R [$F > 4.0\sigma(F)$][a]	0.032	0.042
wR [$F > 4.0\sigma(F)$][b]	0.076	0.091
Goodness-of-fit (GOF)[c]	1.038	0.981
ρ_{max}, ρ_{min} (e Å^{-3})	0.265, −0.383	0.355, −0.312

[a] $R = \sum ||F_o| - |F_c|| / \sum |F_o|$.

[b] $R = \left\{ \sum \left[w(F_o^2 - F_c^2)^2 \right] / \sum \left[w(F_o^2)^2 \right] \right\}^{1/2}$.

[c] The goodness-of-fit (GOF) equals $\left\{ \sum \left[w(F_o^2 - F_c^2)^2 \right] / (N_{rf\ln s} - N_{params}) \right\}^{1/2}$.

Table 2
Crystal data and structure refinement for compounds **1**–**3**.

	1	**2**	**3**
Crystal shape	prism	prism	prism
Color	colorless	colorless	colorless
Size (mm)	0.20 × 0.16 × 0.10	0.39 × 0.33 × 0.24	0.50 × 0.28 × 0.27
Chemical formula	$C_7H_{11}Cl_2N_3OSZn$	$C_9H_{13}Cl_2N_3SZn$	$C_{19}H_{17}Cl_2N_3SZn$
Formula weight	321.52	331.55	455.69
Crystal system	triclinic	triclinic	monoclinic
Space group	$P\bar{1}$	$P\bar{1}$	Cc
Unit cell dimensions			
a (Å)	8.415(2)	8.728(1)	10.213(1)
b (Å)	8.449(2)	9.103(1)	15.117(1)
c (Å)	8.849(2)	9.330(1)	12.244(1)
α (°)	69.288(4)	88.471(2)	
β (°)	79.737(4)	74.254(2)	95.306(2)
γ (°)	79.630(4)	67.540(2)	
Cell volume (Å^3)	574.4(2)	656.9(1)	1882.2(2)
Z	2	2	4
T (K)	110(2)	100(2)	100(1)
D_{calc} (g cm^{-3})	1.859	1.676	1.608
μ (mm^{-1})	2.76	2.41	1.71
F(0 0 0)	324	336	928
θ Range	2.5–26.4	2.3–26.0	0.5–26.0
Index range	$-10 \leqslant h \leqslant 10$, $-9 \leqslant k \leqslant 10$, $0 \leqslant l \leqslant 11$	$-10 \leqslant h \leqslant 10$, $-11 \leqslant k \leqslant 11$, $0 \leqslant l \leqslant 11$	$-12 \leqslant h \leqslant 12$, $0 \leqslant k \leqslant 18$, $-15 \leqslant l \leqslant 15$
Independent reflections	2342	2587	3352
Observed reflections [$F > 4.0\sigma(F)$]	2096 [$F > 4.0\sigma(F)$]	2421 [$F > 4.0\sigma(F)$]	3225 [$F > 4.0\sigma(F)$]
Data completeness	0.994	0.999	1
Maximum/minimum transmission	0.761/0.598	0.595/0.453	0.636/0.568
No. of reflection parameters	144	147	235
R [$F > 4.0\sigma(F)$][a]	0.024	0.020	0.018
wR [$F > 4.0\sigma(F)$][b]	0.058	0.046	0.038
Goodness-of-fit (GOF)[c]	1.041	1.055	0.985
ρ_{max}, ρ_{min} (e Å^{-3})	0.353, −0.385	0.286, −0.328	0.194, −0.245

[a] $R = \sum ||F_o| - |F_c|| / \sum |F_o|$.

[b] $R = \left\{ \sum \left[w(F_o^2 - F_c^2)^2 \right] / \sum \left[w(F_o^2)^2 \right] \right\}^{1/2}$.

[c] The goodness-of-fit (GOF) equals $\left\{ \sum \left[w(F_o^2 - F_c^2)^2 \right] / (N_{rf\ln s} - N_{params}) \right\}^{1/2}$.

displacement parameters for non-hydrogen atoms, except for disordered atoms with isotropic displacement parameters. The crystal structure of the ligand DPhPzTz presented a dynamic disorder affecting the C(22) atom (equivalent to the C(4) atom in Scheme 1 for other independent molecule) that was modellized using two sets of positions. For this procedure the occupancy of two alternate orientations were constrained to unity. The refined occupancy was 83% and 17% for C(22A) and C(22B), respectively. All hydrogen atoms attached to carbon atoms were positioned geometrically, with U_{iso} values derived from U_{eq} values of the corresponding carbon atoms. However, hydrogen atoms of the water molecule were detected by Fourier differences and were refined with fixed O–H and H–H distances (0.957(3) and 1.513(3) Å, respectively). Graphical representations of the molecular structures were generated using ORTEP3 [19] and Mercury [20] for Windows. Experimental details of the crystal structure determinations are listed in Tables 1 and 2.

2.5. Isolation of neutrophils

Neutrophils were isolated by adding in thin glass tubes and in the following order, 2.5 mL of 1119 Histopaque (Sigma–Aldrich) separating medium, 2.5 mL of 1077 Histopaque (Sigma–Aldrich) separating medium and 2.5 mL of human peripheral blood from six healthy volunteers who were not treated with antibiotics, anti-inflammatories or anticoagulants, in order to not affect cell adherence. The samples were then centrifuged at 600*g* for 15 min at room temperature. The halo of neutrophils was withdrawn using a glass Pasteur pipette and washed with PBS medium in plastic tubes. The supernatant was discarded and the tube was beaten so that cells detached. Then, 2 mL of Hank's medium was added and the pellet resuspended. Cells were counted in a Neubauer haemocytometer under phase contrast microscopy at 40×, and the suspension was adjusted to 5×10^5 neutrophils/mL.

2.6. Cell viability assay

Metabolic activity of cells was evaluated using a MTT (3-(4,5-dimethylthiazol-2-yl)-2,5-diphenyltetrazolium bromide) assay. The cells were plated in 96-multiwell plates at a density of 10^5 cells/well and treated with the organic ligands, complexes **1**–**3** and $ZnCl_2$ (in DMSO solutions) in different doses (100 nM, 1, 10 and 100 μM) for 30 min at 37 °C. After the treatment period, MTT (5 mg/mL, 5 μL) was added to each well and incubated for 60 min at 37 °C. After the incubation period, the media were removed and DMSO was added to solubilize the dark blue formazan crystals, and optical density was measured in triplicate in an automatic microplate reader (Tecan Infinite M200) at a test wavelength of 490 nm and reference wavelength of 650 nm. The data are presented as variation above control (untreated samples).

2.7. Phagocytosis of latex beads

Aliquots of 200 μL of Hank's cellular suspension were put into the wells of plastic macrophague migration inhibition factor (MIF)-type plaques (AFORA, Spain), following the method described by Rodríguez et al. [21]. After 30 min incubation at 37 °C in a stove, the adhered monolayer was washed with PBS at 37 °C. Then, 200 L of Hank's medium, 20 L of latex beads (1.1×10^{-3} mm, diluted to 1% in PBS; Sigma) and 3 L of ligand, salt or complex 1×10^{-4} M, yielding a final concentration of 1.3×10^{-3} mM (3 L of DMSO for control) were added, following by

another 30 min incubation at 37 °C in a stove. Finally, the samples were washed with PBS, fixed with methanol 5 min and stained with eosin (five passes) and hematoxylin (five passes). The plaques were carefully rinsed with tap water and dried, followed by counting under oil-immersion phase-contrast microscopy at 100×.

The number of particles ingested per 100 neutrophils was expressed as the latex-bead phagocytosis index (P.I.). The percentage of cells that had phagocytized at least one latex bead was expressed as the phagocytosis percentage (P.P.). The ratio P.I./P.P. was calculated, giving the phagocytosis efficiency (P.E.). Results were referred to 100% of the control to avoid the dispersion due to the great variability of patients' cells phagocytic activity.

2.8. Statistical analysis

The results of the biological study were analyzed using the ANOVA-Scheffe's *F*-test. $P < 0.05$ was considered statistically significant. Data were expressed as the mean (X) ± standard error (SE) of six experiments, performed in duplicate.

3. Results and discussion

3.1. Description of the crystal structures

The single-crystal X-ray diffraction analysis revealed that PzTz crystallizes in the triclinic system with four independent molecules in the asymmetric unit cell, meanwhile the crystal of DPhPzTz is developed into an monoclinic lattice with two compound molecules per unit cell. A diagram of the molecular structure of one molecule with the atom labeling is displayed in Fig. 1 (in the case of PzTz) and Fig. 2 (for DPhPzTz). Likewise, selected interatomic distances and angles are given in Table 3.

In both ligands, in the S(1)–C(1)–N(1)–C(2)–C(3)–C(4) ring (and the equivalent rings in the rest of the independent molecules in the

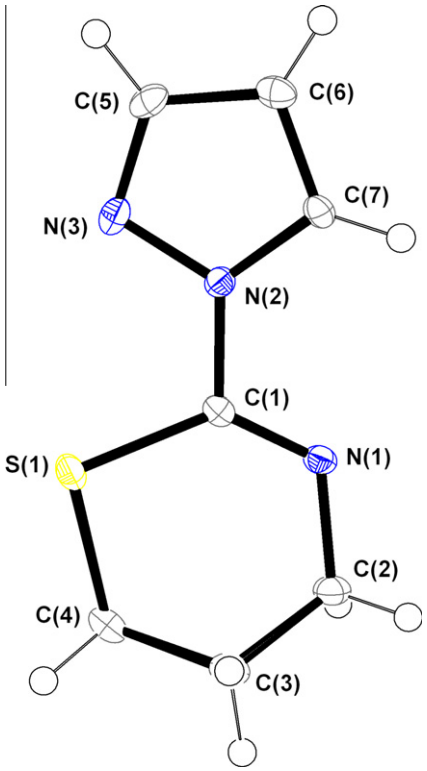

Fig. 1. Crystal structure of one independent molecule of PzTz. The thermal ellipsoids are plotted at the 50% probability level.

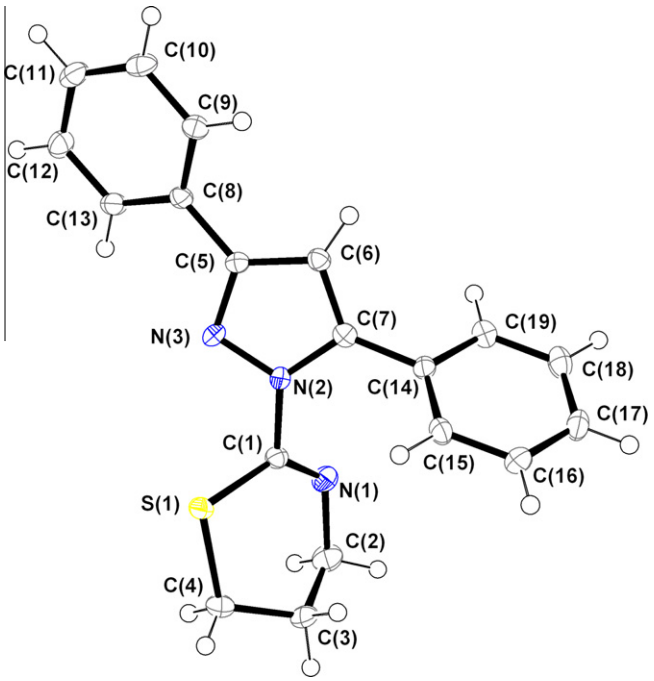

Fig. 2. Crystal structure of one independent molecule of DPhPzTz. The thermal ellipsoids are plotted at the 50% probability level.

Table 3
Selected bond lengths (Å) and angles (°) for ligands PzTz and DPhPzTz.

	PzTz	DPhPzTz		PzTz	DPhPzTz
N(1)–C(1)	1.261(2)	1.254(2)	S(1)–C(1)	1.758(2)	1.762(2)
S(1)–C(4)	1.816(2)	1.828(2)	C(3)–C(4)	1.516(2)	1.516(3)
C(2)–C(3)	1.517(2)	1.512(3)	N(1)–C(2)	1.466(2)	1.469(2)
N(2)–C(1)	1.427(2)	1.432(2)	N(2)–N(3)	1.366(2)	1.366(2)
N(3)–C(5)	1.326(2)	1.334(2)	C(5)–C(6)	1.403(2)	1.410(4)
C(6)–C(7)	1.366(2)	1.369(3)	N(2)–C(7)	1.362(2)	1.367(2)
S(1)–C(1)–N(1)	131.8(1)	131.9(2)	C(1)–N(1)–C(2)	121.4(1)	119.8(2)
N(1)–C(2)–C(3)	116.5(1)	114.4(2)	C(2)–C(3)–C(4)	111.9(1)	111.5(2)
S(1)–C(4)–C(3)	112.1(1)	112.3(1)	C(1)–S(1)–C(4)	98.1(1)	99.6(1)
N(1)–C(1)–N(2)	116.3(1)	117.3(2)	S(1)–C(1)–N(2)	111.8(1)	111.0(1)
C(1)–N(2)–C(7)	126.5(1)	128.0(2)	N(3)–N(2)–C(1)	121.0(1)	119.2(1)
N(3)–N(2)–C(7)	112.4(1)	112.5(2)	N(2)–N(3)–C(5)	103.7(1)	104.5(1)
N(3)–C(5)–C(6)	112.4(1)	111.0(2)	C(5)–C(6)–C(7)	105.1(2)	106.2(2)
N(2)–C(7)–C(6)	106.4(2)	105.8(2)			

Table 4
Selected bond lengths (Å), angles (°) and hydrogen bond parameters for compounds **1**–**3**.

	1	**2**	**3**
Zn–Cl(1)	2.254(1)	2.218(1)	2.213(1)
Zn–Cl(2)	2.296(1)	2.203(1)	2.195(1)
Zn–N(1)	2.200(2)	2.050(1)	2.035(2)
Zn–N(3)	2.072(2)	2.034(1)	2.058(2)
Zn–O(1w)	2.170(2)		
Cl(1)–Zn–Cl(2)	109.0(1)	113.8(1)	120.6(1)
Cl(1)–Zn–N(1)	98.1(1)	121.9(1)	110.4(1)
Cl(1)–Zn–N(3)	137.6(1)	108.4(1)	110.1(1)
N(1)–Zn–Cl(2)	99.5(1)	107.0(1)	112.8(1)
N(3)–Zn–Cl(2)	113.4(1)	123.6(1)	116.7(1)
N(1)–Zn–N(3)	75.1(1)	78.5(1)	78.6(1)
O(1w)–Zn–Cl(1)	94.5(1)		
O(1w)–Zn–Cl(2)	97.3(1)		
O(1w)–Zn–N(1)	154.5(1)		
O(1w)–Zn–N(3)	80.6(1)		
D–H···A	position of A	A···D (Å)	A···H–D (°)
1			
O(1w)–H(1w)···Cl(2)	$-x+1, -y, -z+1$	2.209(20)	169(2)
O(1w)–H(2w)···Cl(1)	$-x, -y+1, -z$	2.277(22)	157(2)

unit cell) the short endocyclic C=N bond is accompanied by a high S–C–N angle and a large S–C(sp^2) bond. This fact is characteristic of a 5,6-dihydro-4H-1,3-thiazine ring [22].

On the other hand, selected bond distances and angles for complex **1** are shown in Table 4. Fig. 3 shows an ORTEP diagram of the molecular structure. In this complex the central zinc ion is five-coordinated by two chloro ligands, one water molecule and two nitrogen atoms from PzTz ligand. In order to determine the geometry around the metallic ion the methods proposed by Addison et al. [23] and by Muetterties and Guggemberger [24] have been applied. The values obtained for parameters τ and Δ were 0.76 and 0.44, respectively, which indicates that the coordination geometry can be described as a highly distorted trigonal bipyramid. The equatorial plane is constituted by atoms Cl(1), Cl(2) and N(3), while the axial positions are occupied by atoms N(1) and O(1w).

The crystal structure of this complex is stabilized by a hydrogen-bond network where the oxygen atom of the water molecule acts as donor of hydrogen while the chloro ligands of neighbor molecules act as acceptors, in such a way that a zigzag chain along the *a* axis is formed (Fig. 4). These chains are linked to each other through van der Waals forces.

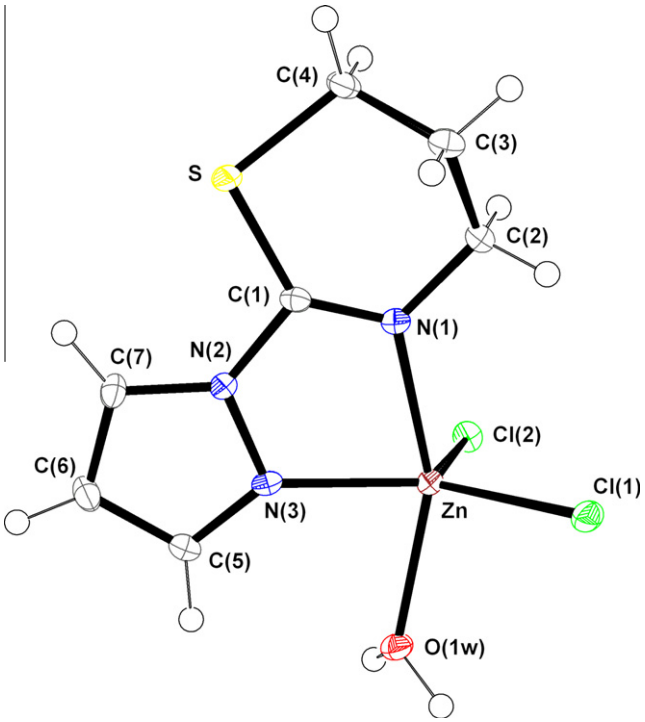

Fig. 3. Crystal structure of **1**. The thermal ellipsoids are plotted at the 50% probability level.

Conversely, the structure of complexes **2** and **3** consists of discrete neutral monomeric units in which the environment around the zinc(II) atom may be described as a distorted tetrahedron. In both complexes the metallic atom is coordinated to two chloro ligands, one thiazinic nitrogen and one pyrazolic nitrogen. A diagram of the molecular structures and the atom numbering system used is represented in Figs. 5 and 6, while the most relevant bond lengths and angles are listed in Table 4.

The difference in the coordination index of the five-coordinated complex **1** and the four-coordinated complexes **2** and **3** could be a consequence of the absence of voluminous substituents in the pyrazole ring of the organic ligand PzTz, which permits the coordination of a higher number of ligands to the metallic ion. Additionally, the distortion of the tetrahedral geometry was expected to be higher in **3** than in **2**, since the steric effects caused by the phenyl substituents should be stronger than the hindrance induced by methyl groups. However, there are not big differences in the distortion of the coordination geometry (dihedral angle between planes Cl(1)–Zn–Cl(2) and N(1)–Zn–N(3) = 77.1° in **2**, 88.4° in **3**) probably due to the fact that the phenyl rings can rotate through C(5)–C(8) and C(7)–C(14) bonds and adopt a position that minimizes the steric hindrance.

Finally, as it can be observed in Figs. 3 and 6, one remarkable difference in complexes **1** and **3** with respect to the structure of their corresponding free ligands PzTz and DPhPzTz is the different degree of rotation of the thiazine ring around C(1)–N(2) bond, which permits the coordination through the thiazine and pyrazole nitrogen atoms [torsion angle N(1)–C(1)–N(2)–N(3) = 165.3° in PzTz, 3.9° in **1**; 123.6° in DPhPzTz, 7.9° in **3**].

3.2. IR spectra

The IR spectra of complexes **1**–**3** showed a strong absorption corresponding to the thiazine ring ν(C=N) vibration (at 1625 cm^{-1} in **1**, 1597 cm^{-1} in **2** and 1635 cm^{-1} in **3**). These bands are shifted negatively relative to the uncoordinated thiazine ring of the respective ligands (1635 cm^{-1} in PzTz, 1639 cm^{-1} in DMPzTz and DPhPzTz). Likewise, the stretching vibrations corresponding to the pyrazole ring shifted to higher wavenumbers compared with those for the respective free ligands. From these facts it can be deduced coordination via the thiazine and pyrazole nitrogen atoms of the ligands [25–27].

In the low-frequency region, some bands due to metal–ligand stretching vibrations are observed. Tentative assignments are listed in Table 5. These bands have been assigned in good agreement with the literature data. In this way, ν(Zn–Cl) vibrations are

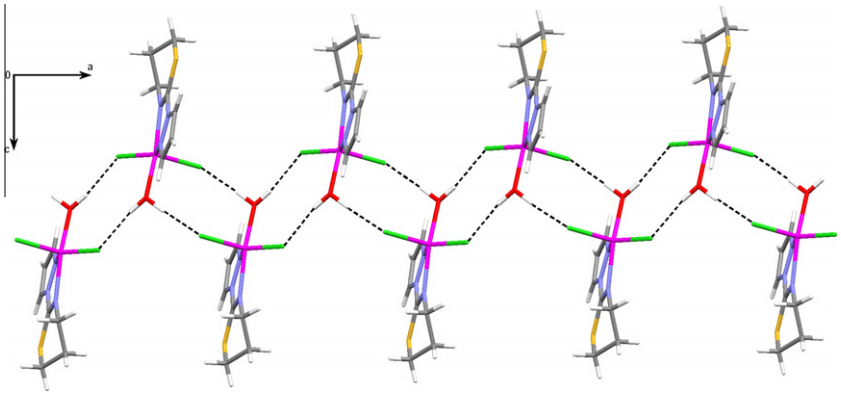

Fig. 4. Hydrogen bonds in the crystal of **1**.

detected in the range 332–214 cm^{-1} [9,28–30]. Likewise, $\nu(Zn–N_{pyrazole})$ vibration is registered in several zinc(II) complexes between 198 and 252 cm^{-1} [31,32], whereas $\nu(Zn–N_{thiazine})$ vibration are assigned in the range 210–250 cm^{-1} in complexes with this type of bond [9,28]. Finally, the $Zn–O_{water}$ stretching vibration is usually detected over 300 cm^{-1} [33,34].

3.3. Mass spectra

The mass spectra for **1**–**3** show signals at *m*/*z* values corresponding to Zn(II)/organic ligand coordinated species. Thus, for **1** a signal at *m*/*z* 168 is due to the ($PzTz^+$) ligand, which is also the base peak of the spectrum. Similarly, the signal at *m*/*z* 269 is

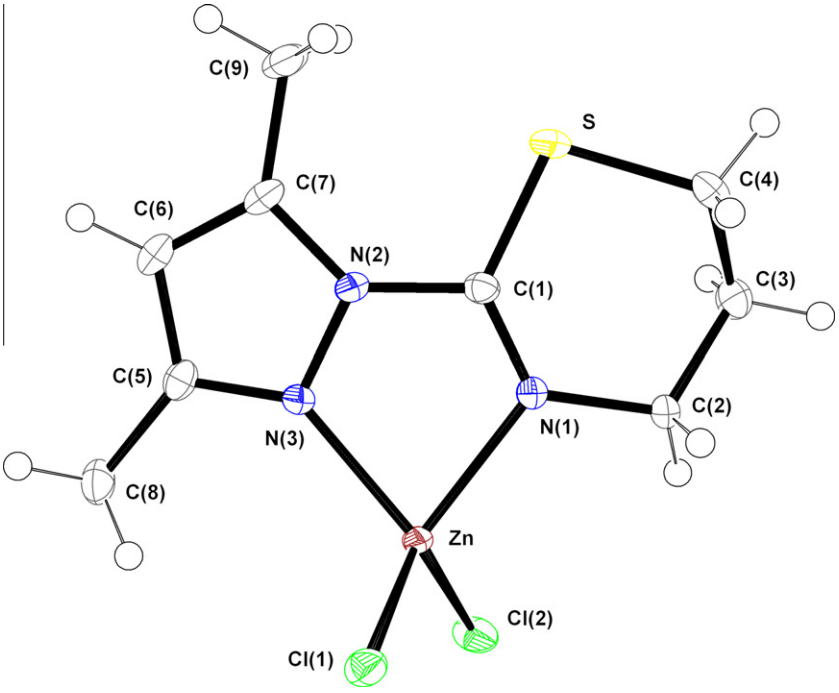

Fig. 5. Crystal structure of **2**. The thermal ellipsoids are plotted at the 50% probability level.

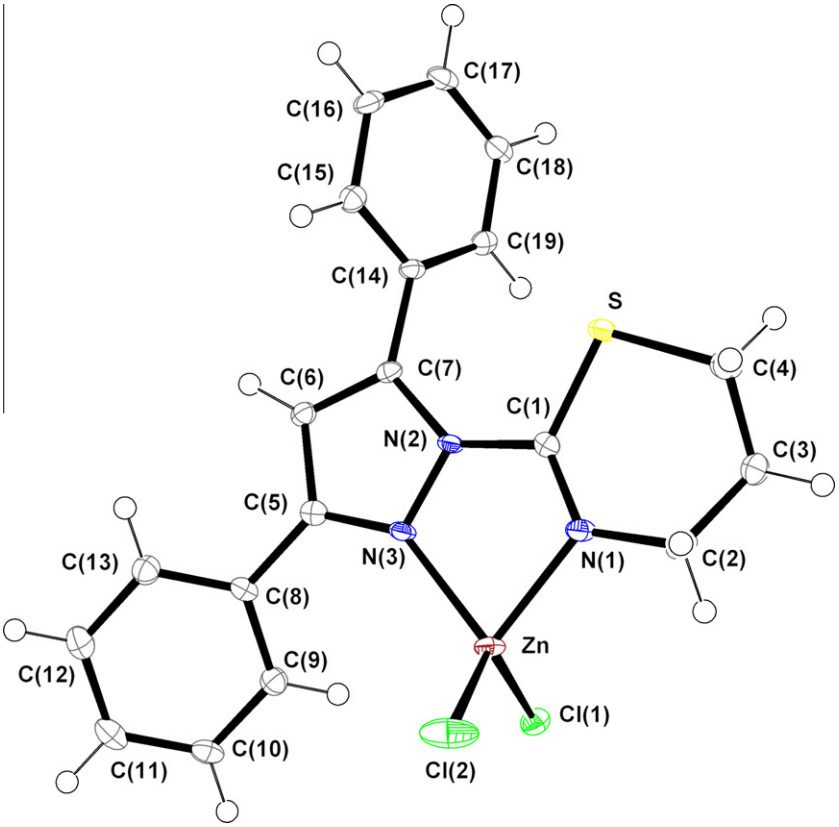

Fig. 6. Crystal structure of **3**. The thermal ellipsoids are plotted at the 50% probability level.

Table 5
Far IR bands for zinc complexes (in cm^{-1}).

	1	2	3
$\nu(Zn–Cl_{terminal})$	308, 291	336, 318	337, 313
$\nu(Zn–N_{pyrazole})$	235	245	244
$\nu(Zn–N_{thiazine})$	220	220	209
$\nu(Zn–OH_2)$	308		

assigned to the $[ZnCl(PzTz)]^+$ fragment, and the signal corresponding to $[ZnCl_2(H_2O)(PzTz)]^+$ appears at *m*/*z* 322. In the case of **2**, the presence of signals at *m*/*z* 196 (corresponding to $DMPzTz^+$) and 332 (assignable to $[ZnCl_2(DMPzTz)]^+$) are registered. Finally, in the spectrum of **3** there is one peak at *m*/*z* 320, which corresponds at the ligand ($DPhPzTz^+$), and another one at *m*/*z* 386, which can be assigned to the $[Zn(DPhPzTz)]^+$ fragment. Besides, no signals corresponding to Zn(II)/DMSO species have been detected. One may

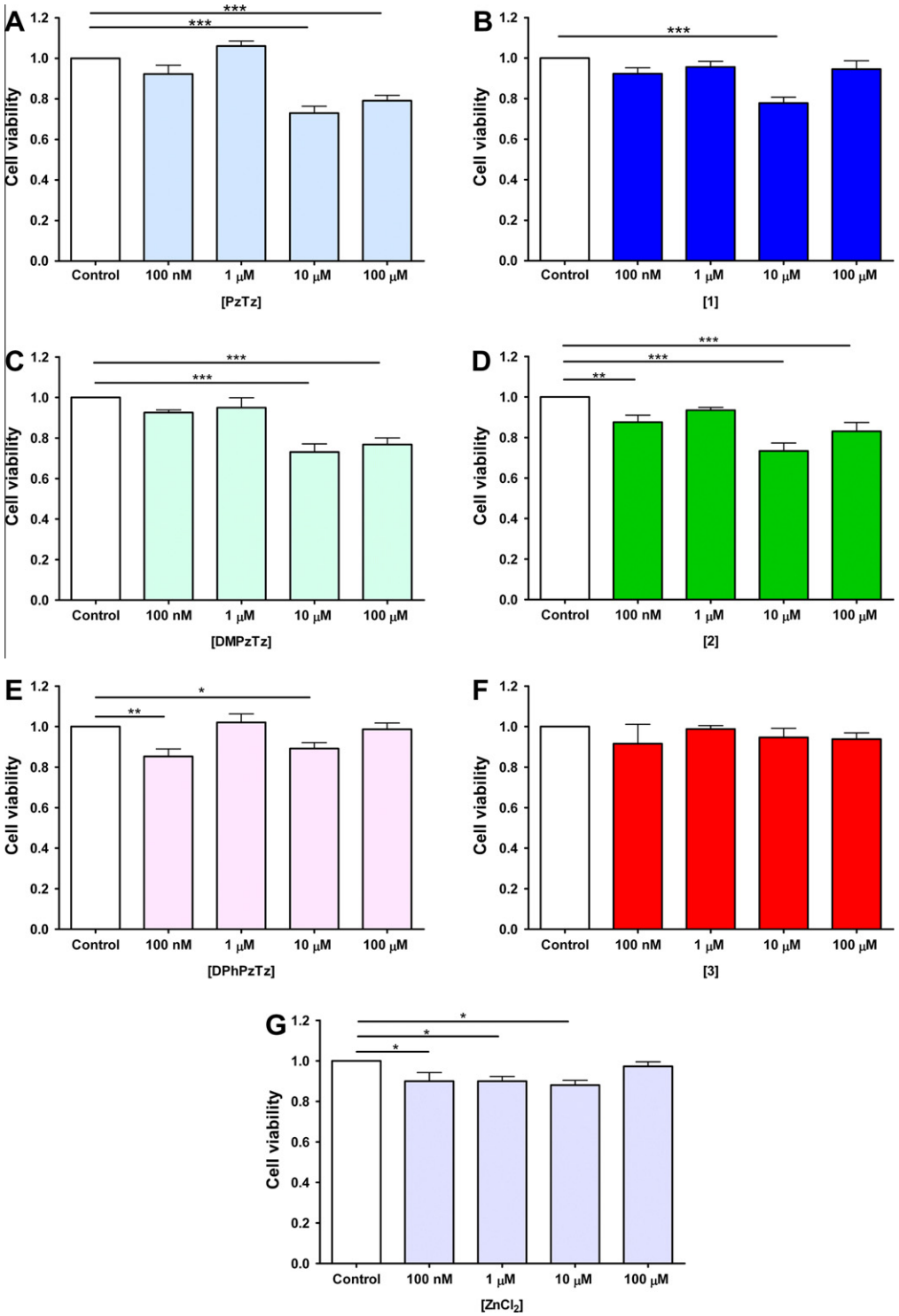

Fig. 7. Cell viability of human neutrophils incubated in the presence of PzTz (A), **1** (B), DMPzTz (C), **2** (D), DPhPzTz (E), **3** (F) and $ZnCl_2$ (G). Each value represents $X \pm SE$ of six determinations performed in triplicate. $^*P < 0.05$; $^{**}P < 0.01$; $^{***}P < 0.001$.

hence deduce from these observations that the coordination of Zn(II) to the organic ligands is maintained in these conditions.

3.4. UV–Vis spectra

The UV–Vis spectra of the ligands, the Zn(II) complexes and $ZnCl_2$ have been recorded in DMSO solution at a concentration of 10^{-5} M. The spectra of complexes **1**–**3** are very similar to those of their respective organic ligands. In PzTz and **1** a single band at 257 nm (ε = 10380 L cm^{-1} mol^{-1} for PzTz and 8090 L cm^{-1} mol^{-1} for **1**) is detected. In DMPzTz and **2** a maximum at 257 nm (ε = 9400 L cm^{-1} mol^{-1} for DMPzTz and 14320 L cm^{-1} mol^{-1} for **2**) with a shoulder at 277 nm (ε = 3750 L cm^{-1} mol^{-1} for DMPzTz and 6120 L cm^{-1} mol^{-1} for **2**) is registered, whereas the spectra of DPhPzTz and **3** consist of a broad band with a maximum at 257 nm (ε = 12340 L cm^{-1} mol^{-1}) for DPhPzTz and at 259 nm (ε = 20000 L cm^{-1} mol^{-1}) for **3**. Finally, in the spectrum of the inorganic salt a maximum is observed at 275 nm (ε = 6650 L cm^{-1} mol^{-1}). This band is not registered in the spectra of **1**–**3**, and so it can be deduced that the structure of the complexes is maintained in DMSO solution.

3.5. Cell viability

The cell viability of human neutrophils when treated with the three organic ligands, complexes **1**–**3** and $ZnCl_2$ have been studied at concentrations of 100 nM, 1, 10 and 100 μM. Fig. 7 shows the results obtained. As can be observed in this figure, cell viability is not strictly dose-dependent. These data confirm that there is not any significant difference in cell viability before and after treatment at a concentration below 10 μM, according to Scheffe *F*-test, except in the case of complex **2**, ligand DPhPzTz and $ZnCl_2$, which present significant fall at a concentration of 100 nM. In all cases, the cell viability with respect to the control sample at a concentration of 1 μM was above 85%. This suggest that the treatment with PzTz, DMPzTz, DPhPzTz, **1**, **2**, **3** and $ZnCl_2$ does not cause any cellular damage under the work conditions and during the time our experiments lasted. Therefore, the optimal concentration chosen to perform the phagocytosis studies reported in this work was 1 μM.

3.6. Study of the phagocytic function

The capacity of neutrophils to ingest latex beads, expressed as the phagocytosis index (Fig. 8A) increases as consequence of the treatment of neutrophils with our compounds. This growth is statistically significant ($P < 0.001$) in the case of cells treated with **1**, **2** and **3** in comparison with the control sample and with the sample treated with the Zn(II) salt. Likewise, the samples treated with zinc complexes **1**–**3** present a statistically significant growth ($P < 0.01$ or $P < 0.001$) with respect to their respective organic ligands. Regarding the phagocytic percentage (Fig. 8B) no significant differences have been found in samples treated with complexes with respect to control and the samples treated with the organic ligands and the inorganic salt. Finally, in the case of phagocytic efficiency (Fig. 8C), this is significantly higher in cells treated with **1**–**3** ($P < 0.001$) compared with control and $ZnCl_2$. Besides, this parameter is also significantly greater than the corresponding ligands in all complexes.

From these results it is demonstrated that coordination to zinc(II) improves neutrophils function, enhancing the non-specific immune response, since phagocytosis index and phagocytic efficiency are higher in the case of samples treated with **1**, **2** and **3** with respect to the samples to which the organic ligands or the Zn(II) salt were added. However, substituents in the organic ligands seem to have no influence in the phagocyting capacity of neutrophils, since no statistically significant differences have been found in the biological activity of cells treated with the three Zn(II) complexes.

With respect to the results obtained for the zinc(II) complex [$ZnCl_2$(TzTz)], previously reported [9] (see Fig. 8), this latter compound shows a significantly greater phagocytosis percentage than complexes **1**–**3** and a significantly lower phagocytic efficiency than **2**, while the phagocytosis index does not present significant differences among all complexes. Therefore, it could be deduced that in [$ZnCl_2$(TzTz)] the phagocytosis promoting effect (reflected in the phagocytosis index) is due mainly to active phagocytes number increase (phagocytosis percentage), while in **2** the main factor is the greater efficiency of these active cells phagocytizing antigenic particles (phagocytic efficiency). This different biologic behavior could

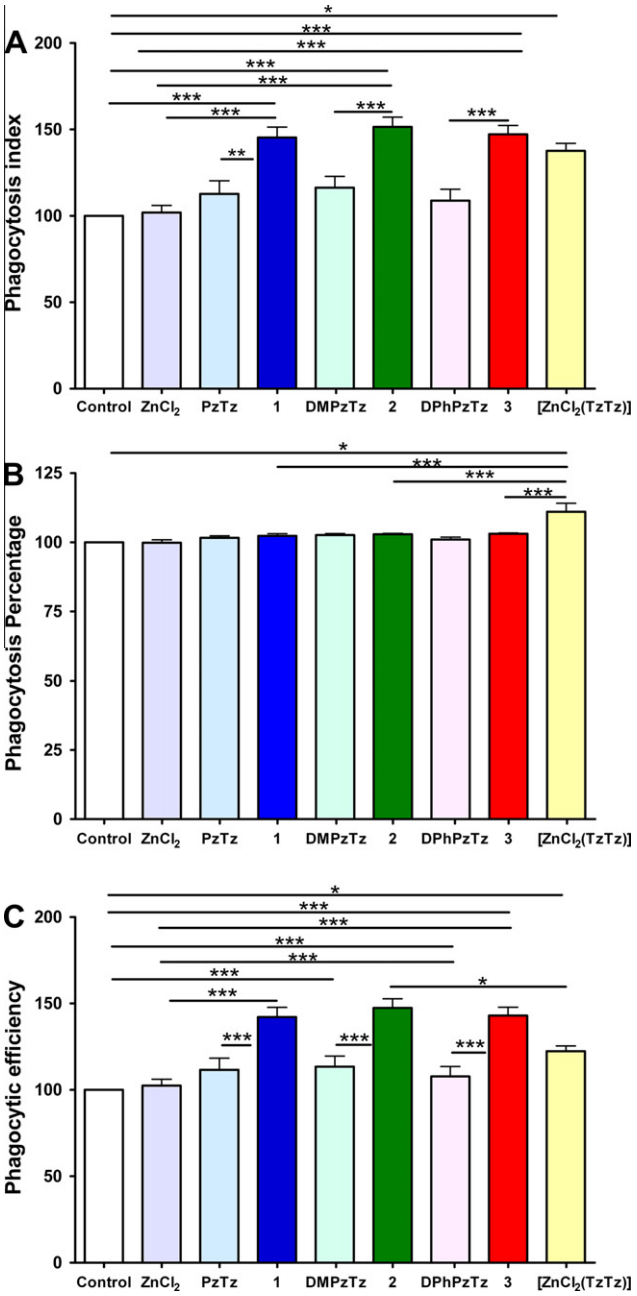

Fig. 8. Phagocytosis index (A), phagocytosis percentage (B) and phagocytic efficiency (C) variations of human neutrophils treated with $ZnCl_2$, PzTz, DMPzTz, DPhPzTz, **1**, **2**, **3** and [$ZnCl_2$(TzTz)] and incubated in the presence of latex beads. Each value represents $X \pm$ SE of six determinations performed in duplicate. $^{*}P < 0.05$; $^{**}P < 0.01$; $^{***}P < 0.001$.

be related to the structural differences between [$ZnCl_2$(TzTz)] and the three complexes studied in this work (e.g. the size of the chelate ring), which are a consequence of the presence of structurally different ligands as TzTz on one hand, and PzTz, DMPzTz and DPhPzTz on the other hand. These differences could affect the assimilation of the compound by the cell and, by extension, the influence of the complex in the cell biologic activity.

Acknowledgements

The authors would like to thank the Junta de Extremadura (III PRI + D + I) and the FEDER (Project PRI08A022) for financial support. J. Espino is beneficiary of a grant from MEC (AP2009-0753).

Appendix A. Supplementary data

CCDC 819474, 819475, 819476, 819477 and 819478 contain the supplementary crystallographic data for this paper. These data can be obtained free of charge via http://www.ccdc.cam.ac.uk/conts/retrieving.html, or from the Cambridge Crystallographic Data Centre, 12 Union Road, Cambridge CB2 1EZ, UK; fax: (+44) 1223-336-033; or e-mail: deposit@ccdc.cam.ac.uk.

References

[1] E. Muñoz, R. Cedeño, J. Rodríguez, W.P.W. Van der Knapp, E. Mialhe, E. Bachère, Aquaculture 191 (2000) 89.
[2] E. Bachere, E. Mialhe, J. Rodríguez, Fish Shellfish Immunol. 5 (1995) 597.
[3] E. Mocchegiani, M. Muzzioli, C. Cipriano, R. Giacconi, Mech. Ageing Dev. (1998) 183.
[4] Ü.S. Gürer, P. Göçer, E. Erçağ, N. Erten, E. Rayaman, B. Gürbüz, A. Üzer, A. Karan, A. Çevikbaş, Int. Immunopharmacol. 6 (2006) 808.
[5] E.S. Wintergest, S. Maggini, D.H. Hornig, Ann. Nutr. Metab. 50 (2006) 85.
[6] T.E. DeCoursey, FEBS Lett. 555 (2003) 57.
[7] M. Konstandinidou, A. Kourounakis, M. Yiangou, L. Hadjipetrou, D. Kovala-Demertzi, S. Hadjikakou, M. Demertzis, J. Inorg. Biochem. 70 (1998) 63.
[8] M. Navarro, I. Colmenares, H. Correia, A. Hernández, Y. Ching, Y. Millán, L.E. Ojeda, M. Velásquez, G. Fraile, Arzneimittel-Forsch. 54 (2004) 746.
[9] F.J. Barros-García, A. Bernalte-García, A.M. Lozano Vila, F. Luna-Giles, J.A. Pariente, R. Pedrero-Marín, A.B. Rodríguez, J. Inorg. Biochem. 100 (2006) 1861.
[10] E. Viñuelas-Zahínos, F. Luna-Giles, P. Torres-García, A.B. Rodríguez, A. Bernalte-García, Inorg. Chim. Acta 366 (2011) 373.
[11] A.M. Lozano-Vila, F. Luna-Giles, E. Viñuelas-Zahínos, F.L. Cumbrera, A.L. Ortiz, F.J. Barros-García, A.B. Rodríguez, Inorg. Chim. Acta 365 (2011) 282.
[12] T.D. Pennig, J.J. Talley, S.R. Bertenshaw, J.S. Carter, P.W. Collins, S. Docter, M.J. Graneto, L.F. Lee, J.W. Malecha, J.M. Miyashiro, R.S. Rogers, D.J. Rogier, S.S. Yu, G.D. Anderson, E.G. Burton, J.N. Cogburn, S.A. Gregory, C.M. Koboldt, W.E. Perkins, K. Seibert, A.W. Veenhuizen, Y.Y. Zhang, P.C. Isakson, J. Med. Chem. 40 (1997) 1347.
[13] S.H. Kim, H. Son, G. Nam, D.Y. Chi, J.H. Kim, Bioorg. Med. Chem. Lett. 10 (2000) 1143.
[14] H.W. Schubert, O. Behner, Arch. Pharm. 301 (1968) 750.
[15] Bruker AXS Inc., SADABS, Version 2.03 Bruker AXS Inc., Madison, WI, 2001.
[16] M. Sheldrick, SHELXS-97, Program for Crystal Structures Solution, University of Göttingen, Germany, 1997.
[17] M. Sheldrick, SHELXL-97, Program for Crystal Structures Refinement, University of Göttingen, Germany, 1997.
[18] L.J. Farrugia, J. Appl. Crystallogr. 32 (1999) 837.
[19] L.J. Farrugia, J. Appl. Crystallogr. 30 (1997) 565.
[20] C.F. Macrae, I.J. Bruno, J.A. Chisholm, P.R. Edgington, P. McCabe, E. Pidcock, L. Rodriguez-Monge, R. Taylor, J. van de Streek, P.A. Wood, J. Appl. Crystallogr. 41 (2008) 466.
[21] A.B. Rodríguez, C. Barriga, M. De La Fuente, Agents Act. 31 (1990) 86.
[22] G. Argay, A. Kalman, A. Kapor, B. Ribar, Acta Crystallogr. B36 (1980) 363.
[23] A.W. Addison, T.N. Rao, J. Reedijk, J. Van Rijn, G.C. Verschoor, J. Chem. Soc., Dalton Trans. (1984) 1349.
[24] E.L. Muetterties, J. Guggemberger, J. Am. Chem. Soc. 96 (1974) 1748.
[25] M. Shakir, S.P. Vakey, F. Firdaus, P.S. Hameed, Polyhedron 13 (1994) 2319.
[26] B. Singh, R.N. Singh, R.C. Aggarwal, Polyhedron 4 (1985) 401.
[27] M.G. Abd El-Wahed, M.S. Refat, S.M. El-Megharbel, Mol. Struct. 888 (2008) 416.
[28] A. Bernalte-García, F.J. Barros-García, F.J. Higes-Rolando, F. Luna-Giles, Polyhedron 20 (2001) 3315.
[29] R. López-Garzón, M.D. Gutiérrez-Valero, M.L. Rodino-Salido, A. Sánchez-Rodrigo, M. Nogueras-Montiel, J.M. Moreno, R. Odedra, K.H.A.M. El-Bayouki, Inorg. Chim. Acta 258 (1997) 33.
[30] E. Viñuelas-Zahínos, F. Luna-Giles, P. Torres-García, A. Bernalte-García, Polyhedron 28 (2009) 4056.
[31] A. Cingolani, D. Martín, F. Marchetti, C. Pettinari, M. Ricciutelli, B.W. Skelton, A.H. White, Inorg. Chim. Acta 350 (2003) 641.
[32] A. Kovács, K.M. Szécsényi, V.M. Leovac, Z.D. Tomić, G. Pokol, J. Organomet. Chem. 692 (2007) 2582.
[33] M.A. Maldonado-Rogado, E. Viñuelas-Zahínos, F. Luna-Giles, F.J. Barros-García, Polyhedron 26 (2007) 5210.
[34] J.R. Ferraro, Low-Frequency Vibrations of Inorganic and Coordination Compounds, Plenum Press, New York, 1971.